


# Nonparaxial propagation of radially polarized chirped Airy beams in uniaxial crystal orthogonal to the optical axis

Yaohui Chen(陈耀辉), Lixun Wu(吴理汛), Zhixiong Mo(莫智雄), Lican Wu(吴利灿), and Dongmei Deng(邓冬梅)
**Citation:**Chin. Phys. B, 2021, 30 (**1**): 014204. DOI: 10.1088/1674-1056/abb226
Journal homepage: http://cpb.iphy.ac.cn; http://iopscience.iop.org/cpb

**What follows is a list of articles you may be interested in**

---

## Hyperbolic metamaterials for high-efficiency generation of circularly polarized Airy beams

Lin Chen(陈林), Huihui Li(李会会), Weiming Hao(郝玮鸣), Xiang Yin(殷祥), Jian Wang(王健)
Chin. Phys. B, 2020, 29 (**8**): 084210. DOI: 10.1088/1674-1056/ab96a1

## Three-Airy autofocusing beams

Xiao-Hong Zhang(张小红), Fei-Li Wang(王飞利), Lu-Yang Bai(白露阳), Ci-Bo Lou(楼慈波), Yi Liang(梁毅)
Chin. Phys. B, 2020, 29 (**6**): 064204. DOI: 10.1088/1674-1056/ab84d2

## Comparison of three kinds of polarized Bessel vortex beams propagating through uniaxial anisotropic media

Jia-Wei Liu(刘佳伟), Hai-Ying Li(李海英), Wei Ding(丁炜), Lu Bai(白璐), Zhen-Sen Wu(吴振森), Zheng-Jun Li(李正军)
Chin. Phys. B, 2019, 28 (**9**): 094214. DOI: 10.1088/1674-1056/ab37f5

## Nonparaxial propagation properties of the chirped Airy Gaussian vortex beams in uniaxial crystals orthogonal to the optical axis

Yizuo Chen(陈奕佐), Guanwen Zhao(赵官文), Feng Ye(叶峰), Chuangjie Xu(许创杰), Dongmei Deng(邓冬梅)
Chin. Phys. B, 2018, 27 (**10**): 104201. DOI: 10.1088/1674-1056/27/10/104201

## Experimental verification on tightly focused radially polarized vortex beams

Du Fu-Rong, Zhou Zhe-Hai, Tan Qiao-Feng, Yang Chang-Xi, Zhang Xiao-Qing, Zhu Lian-Qing
Chin. Phys. B, 2013, 22 (**6**): 064202. DOI: 10.1088/1674-1056/22/6/064202

---

# Nonparaxial propagation of radially polarized chirped Airy beams in uniaxial crystal orthogonal to the optical axis*

Yaohui Chen(陈耀辉), Lixun Wu(吴理汛), Zhixiong Mo(莫智雄), Lican Wu(吴利灿), and Dongmei Deng(邓冬梅)†

*Guangdong Provincial Key Laboratory of Nanophotonic Functional Materials and Devices, South China Normal University, Guangzhou* 510631, *China*

(Received 2 July 2020; revised manuscript received 12 July 2020; accepted manuscript online 25 August 2020)

The nonparaxial propagation of radially polarized chirped Airy beams (RPCAiBs) in uniaxial crystal orthogonal to the optical axis is analytically studied. The effects of the first and the second order chirp factors, and the ratio of the extraordinary refractive index to the ordinary refractive index on the nonparaxial evolution of RPCAiBs in different observation planes are investigated in detail. The results show that when one parameter changes, different components behave differently, and even the same component has various behavior in different directions. The initial slope of RPCAiBs in the *x*-direction varies more with the first order chirp factor than that in the *y*-direction. Meanwhile, with the second order chirp factor becoming larger, the depth of the focus of the *y*-component in the *x*-direction decreases while that in the *y*-direction has no difference. In addition, the different ratios of the extraordinary refractive index to the ordinary refractive index change the difference of the depth of the focus between the *x*- and the *y*-components.

**Keywords:** radial polarization, nonparaxial propagation, Airy beam, uniaxial crystal, chirp

**PACS:** 42.65.–k **DOI:** 10.1088/1674-1056/abb226

## 1. Introduction

In 1979, as the fact that the Airy function is a solution to the Schrödinger equation was demonstrated by Berry and Balazs, an Airy wave packet was predicted theoretically.[1] Although the Airy wave also has the characteristics of self-healing and self-accelerating, it is not physically realizable because of its infinite energy. Since the intensive research and experimental demonstration on the Airy beams with finite energy were conducted by Siviloglou and Christodoulides in 2007,[2,3] the Airy beam has attracted tremendous attention because of its special characteristics such as self acceleration,[2,3] nondiffraction[4] and self-healing.[5] In the last decades, the Airy beam has been applied in many areas[6] such as the optical cleaning of the micro particles,[7] the light-sheet microscopy,[8] the light bullet generation[9,10] and the curved plasma channel generation.[11,12] Recently, some new types of the auto-focusing beam have been reported[13,14] and a kind of novel property of the Airy-like beam has been investigated.[15,16]

So far, researchers have diffusely studied the paraxial propagation of Airy beams in media with external potentials,[17–19] inhomogeneous medium,[20–24] linear medium,[4,5] nonlinear medium[25,26] and apertured optical system.[27] Researches on the propagation of laser beams in uniaxial crystals have important effects on the design of compensators, polarizers, amplitude and phase modulation devices.[28–30] However, the theory of paraxial propagation is no longer applicable when the beam waist radius is equivalent to the wavelength in a uniaxial crystal or the far-field divergence angle is large. In this case, the nonparaxial effects of the beam should be concentrated on. Varieties of nonparaxial methods have been developed to deal with beam propagation beyond the paraxial approximation.[31–34] In particular, a practical method is to solve the nonparaxial propagation of laser beams in uniaxial crystals by solving the boundary conditions of Maxwell's equations.[29,30,35,36]

Since 2007, the first realization of the finite-energy Airy beams has been given,[2] an analytical vectorial structure of radially polarized light beams has been investigated[37] and a review on cylindrical vector beams has been written.[38] For their interesting properties, the radially polarized beams have been applied in different aspects such as optical microfabrication,[39] high-resolution microscopy,[40] acceleration techniques,[41,42] particularly material processing[43,44] and particles guiding or trapping.[45–47] Also, some researches on the propagation of radially polarized Airy beams have been reported in recent years.[48–51] Although the way of strengthening the longitudinal component of the electric field to reduce the size of the light spot does not work in crystals,[52–54] it is still valuable to study the radial polarization in uniaxial crystals due to the interesting effects given in the works.[55,56] On the other hand, the chirp parameter is regarded as a powerful tool in the generation and the manipulation of optical beams.[57,58] Zhang *et al.* studied the impacts of the first and the second order chirp on initial finite energy Airy beams.[18] Therefore, some novel phenomena may be discovered by combining the radial polarization, nonparaxial propagation and chirped Airy beams in uniaxial crystals.

*Projected supported by the National Natural Science Foundation of China (Grant Nos. 11775083 and 11374108), the Science and Technology Program of Guangzhou Province, China (Grant No. 2019050001), and the Special Funds for the Cultivation of Guangdong College Students' Scientific and Technological Innovation, China (Grant No. pdjh2020a0149).

†Corresponding author. E-mail: dmdeng@263.net

© 2021 Chinese Physical Society and IOP Publishing Ltd 

In this paper, we investigate the nonparaxial propagation properties of Airy beams with the first and the second order chirps in uniaxial crystal orthogonal to the optical axis, respectively. The intensity evolutions and transverse intensity of RPCAiBs are analyzed in detail. Based on the results obtained,[59,60] we pay more attention to the different behaviors of the $x$- and the $y$-components and some interesting results are found.

The organization of the paper is as follows. In Section 2, the theoretical model for the nonparaxial propagation in uniaxial crystal orthogonal to the optical axis is presented and we derive analytical solutions of RPCAiBs. In Section 3, the nonparaxial evolutions and transverse intensity of RPCAiBs with the first and the second order chirp factors and the ratios of the extraordinary refractive index to the ordinary refractive index which can be adjusted by using the electro-optical crystal are analyzed. Finally, some useful results are summarized in Section 4.

## 2. Analytic solution of RPCAiBs in uniaxial crystals orthogonal to the optical axis

In the Cartesian coordinate system, the propagation axis is set as the $z$-axis and the optical axis of the uniaxial crystal is the $x$-axis. The relative dielectric tensors $\varepsilon$ of the uniaxial crystal can be expressed as[30]

$$\varepsilon = \begin{pmatrix} n_{\mathrm{e}}^2 & 0 & 0 \\ 0 & n_{\mathrm{o}}^2 & 0 \\ 0 & 0 & n_{\mathrm{o}}^2 \end{pmatrix}, \tag{1}$$

where $n_{\mathrm{o}}$ and $n_{\mathrm{e}}$ are the ordinary and the extraordinary refractive indices of the uniaxial crystal. We assume that RPCAiBs in the $x$-direction is incident on the uniaxial crystal at the initial plane $z = 0$. Therefore, the electric field distribution of RPCAiBs in the input plane can be expressed as

$$\begin{bmatrix} E_x(x_0, y_0, 0) \\ E_y(x_0, y_0, 0) \end{bmatrix} = \begin{bmatrix} \dfrac{x_0}{w_0} Ai\left(\dfrac{x_0}{w_0}\right) Ai\left(\dfrac{y_0}{w_0}\right) \exp\left(\dfrac{ax_0 + ay_0}{w_0} + \mathrm{i}\beta_{1x}\dfrac{x_0}{w_0} + \mathrm{i}\beta_{2x}\dfrac{x_0^2}{w_0^2} + \mathrm{i}\beta_{1y}\dfrac{y_0}{w_0} + \mathrm{i}\beta_{2y}\dfrac{y_0^2}{w_0^2}\right) \\ \dfrac{y_0}{w_0} Ai\left(\dfrac{x_0}{w_0}\right) Ai\left(\dfrac{y_0}{w_0}\right) \exp\left(\dfrac{ax_0 + ay_0}{w_0} + \mathrm{i}\beta_{1x}\dfrac{x_0}{w_0} + \mathrm{i}\beta_{2x}\dfrac{x_0^2}{w_0^2} + \mathrm{i}\beta_{1y}\dfrac{y_0}{w_0} + \mathrm{i}\beta_{2y}\dfrac{y_0^2}{w_0^2}\right) \end{bmatrix}, \tag{2}$$

where $w_0$ denotes the initial length size; $a$ is the truncation factor of the RPCAiBs; $Ai(\cdots)$ represents the first kind of the Airy function; $\beta_{1x}$ and $\beta_{1y}$ are the first order chirp parameters, while $\beta_{2x}$ and $\beta_{2y}$ are the second order chirp parameters.

Under the theory of the nonparaxial propagation in uniaxial crystal orthogonal to the optical axis, the electric field of a beam in uniaxial crystal orthogonal to the optical axis can be expressed as[30]

$$\begin{aligned} \boldsymbol{E}(x,y,z) = & \int\int \mathrm{d}^2\boldsymbol{k}_\perp \exp(\mathrm{i}\boldsymbol{k}_\perp \cdot \boldsymbol{r}_\perp + \mathrm{i}k_{\mathrm{e}z}z) \\ & \times \begin{pmatrix} \tilde{E}_x(\boldsymbol{k}_\perp) \\ -\dfrac{k_x k_y}{k_0^2 n_{\mathrm{o}}^2 - k_x^2}\tilde{E}_x(\boldsymbol{k}_\perp) \\ -\dfrac{k_{\mathrm{e}z}k_x}{k_0^2 n_{\mathrm{o}}^2 - k_x^2}\tilde{E}_x(\boldsymbol{k}_\perp) \end{pmatrix} \\ & + \int\int \mathrm{d}^2\boldsymbol{k}_\perp \exp(\mathrm{i}\boldsymbol{k}_\perp \cdot \boldsymbol{r}_\perp + \mathrm{i}k_{\mathrm{o}z}z) \\ & \times \begin{pmatrix} 0 \\ -\dfrac{k_x k_y}{k_0^2 n_{\mathrm{o}}^2 - k_x^2}\tilde{E}_x(\boldsymbol{k}_\perp) + \tilde{E}_y(\boldsymbol{k}_\perp) \\ -\dfrac{k_y}{k_{\mathrm{o}z}}\left[\dfrac{k_x k_y}{k_0^2 n_{\mathrm{o}}^2 - k_x^2}\tilde{E}_x(\boldsymbol{k}_\perp) + \tilde{E}_y(\boldsymbol{k}_\perp)\right] \end{pmatrix}, \end{aligned} \tag{3}$$

with $k_{\mathrm{e}z}$ and $k_{\mathrm{o}z}$ defined by

$$\begin{aligned} k_{\mathrm{e}z} &= \left[k^2 n_{\mathrm{e}}^2 - \left(\frac{n_{\mathrm{e}}^2}{n_{\mathrm{o}}^2}\right)k_x^2 - k_y^2\right]^{\frac{1}{2}}, \\ k_{\mathrm{o}z} &= (k^2 n_{\mathrm{o}}^2 - k_x^2 - k_y^2)^{\frac{1}{2}}, \end{aligned} \tag{4}$$

where $\boldsymbol{k}_\perp = k_x\hat{e}_x + k_y\hat{e}_y$, $\boldsymbol{r}_\perp = r_x\hat{e}_x + r_y\hat{e}_y$; and $\hat{e}_x$, $\hat{e}_y$ represent the unit vectors along the $x$-direction and the $y$-direction, respectively; $\mathrm{d}^2\boldsymbol{k}_\perp = \mathrm{d}k_x\mathrm{d}k_y$, and $k = \frac{2\pi}{\lambda}$ is the wave number with $\lambda$ being the wavelength of the incident beam in vacuum.

When the evolution of the field in uniaxial crystal is beyond the paraxial approximation, Eq. (3) can be written as the sum of the dominant paraxial term and the nonparaxial correction[30]

$$\begin{aligned} \boldsymbol{E}(x,y,z) = & \exp(\mathrm{i}k_0 n_{\mathrm{e}} z)\int\int \mathrm{d}^2\boldsymbol{k}_\perp \exp[\mathrm{i}(k_x x + k_y y)]\exp\left(-\mathrm{i}\frac{n_{\mathrm{e}}^2 k_x^2 + n_{\mathrm{o}}^2 k_y^2}{2k_0 n_{\mathrm{e}} n_{\mathrm{o}}^2}z\right) \begin{pmatrix} \tilde{E}_x(\boldsymbol{k}_\perp) \\ -\dfrac{k_x k_y}{k_0^2 n_{\mathrm{o}}^2}\tilde{E}_x(\boldsymbol{k}_\perp) \\ -\dfrac{n_{\mathrm{e}}k_x}{k_0 n_{\mathrm{o}}^2}\tilde{E}_x(\boldsymbol{k}_\perp) \end{pmatrix} \\ & + \exp(\mathrm{i}k_0 n_{\mathrm{o}} z)\int\int \mathrm{d}^2\boldsymbol{k}_\perp \exp[\mathrm{i}(k_x x + k_y y)]\exp\left(-\mathrm{i}\frac{k_x^2 + k_y^2}{2k_0 n_{\mathrm{o}}}z\right) \begin{pmatrix} 0 \\ -\dfrac{k_x k_y}{k_0^2 n_{\mathrm{o}}^2}\tilde{E}_x(\boldsymbol{k}_\perp) + \tilde{E}_y(\boldsymbol{k}_\perp) \\ -\dfrac{k_y}{k_0 n_{\mathrm{o}}}\tilde{E}_y(\boldsymbol{k}_\perp) \end{pmatrix}. \end{aligned} \tag{5}$$

Utilizing the properties of Fourier transforms,[61] the electric field of the beams can be written as the three components:[30]

$$E_x(x,y,z) = \frac{kn_o}{2\pi iz}\int\int_{-\infty}^{+\infty} E_x(x_0,y_0,0)A_e(r,r_0)\mathrm{d}x_0\mathrm{d}y_0, \quad (6)$$

$$E_y(x,y,z) = \frac{ikn_o}{2\pi iz^3}\int\int_{-\infty}^{+\infty}(x-x_0)(y-y_0)E_x(x_0,y_0,0) \times [A_e(r,r_0)-A_o(r,r_0)]\mathrm{d}x_0\mathrm{d}y_0 + \frac{kn_o}{2\pi iz}\int\int_{-\infty}^{+\infty} E_y(x_0,y_0,0)A_o(r,r_0)\mathrm{d}x_0\mathrm{d}y_0, \quad (7)$$

$$E_z(x,y,z) = \frac{ikn_o}{2\pi iz^2}\int\int_{-\infty}^{+\infty}[(x-x_0)E_x(x_0,y_0,0)A_e(r,r_0) + (y-y_0)E_y(x_0,y_0,0)A_o(r,r_0)]\mathrm{d}x_0\mathrm{d}y_0, \quad (8)$$

where

$$A_e(r,r_0) = \exp(ikn_e z)\exp\left\{-\frac{k}{2izn_e}[n_o^2(x-x_0)^2+n_e^2(y-y_0)^2]\right\}, \quad (9)$$

$$A_o(r,r_0) = \exp(ikn_e z)\exp\left\{-\frac{kn_o}{2iz}[(x-x_0)^2+(y-y_0)^2]\right\}. \quad (10)$$

Substituting Eqs. (1) and (2) into Eqs. (6)–(8), we obtain

$$E_x(x,y,z) = \frac{kn_o}{2\pi izw_0}\exp(ikn_e z)\exp(-\frac{kn_o^2x^2}{2izn_e}-\frac{kn_e y^2}{2iz})L_1K_1, \quad (11)$$

$$E_y(x,y,z) = \frac{kn_o}{2\pi izw_0}\exp(ikn_e z)\exp\left[-\frac{kn_o(x^2+y^2)}{2iz}\right]L_3K_4 + \frac{ikn_o}{2\pi w_0z^3}[\exp(ikn_e z)\exp\left(-\frac{kn_o^2x^2}{2izn_e}-\frac{kn_e y^2}{2iz}\right)(xyL_1K_2 - xL_1L_2 - yK_2M_1 + M_1L_2) - \exp(ikn_e z)\exp\left[-\frac{kn_o(x^2+y^2)}{2iz}\right](xyL_4K_3 - xL_3L_4 - yK_3M_4 + L_3M_4)], \quad (12)$$

$$E_z(x,y,z) = \frac{ikn_o}{2\pi w_0z^2}\left[\exp(ikn_e z)\exp\left(-\frac{kn_o^2x^2}{2izn_e}-\frac{kn_e y^2}{2iz}\right)(xL_1K_1 - K_1M_1) + w_0\exp(ikn_e z)\exp\left[-\frac{kn_o(x^2+y^2)}{2iz}\right](yL_3K_4 - K_4M_3)\right], \quad (13)$$

where

$$K_n = \sqrt{-\frac{\pi}{b_n}}\exp\left(-\frac{c_n^2}{4b_n}+\frac{c_n}{8w_0^3b_n^2}-\frac{1}{96w_0^6b_n^3}\right)Ai(f_n), \quad (14)$$

$$L_n = \sqrt{-\frac{\pi}{b_n}}\exp\left(-\frac{c_n^2}{4b_n}+\frac{c_n}{8w_0^3b_n^2}-\frac{1}{96w_0^6b_n^3}\right) \times\left[\left(-\frac{c_n}{2b_n}+\frac{1}{8w_0^3b_n^2}\right)Ai(f_n)-\frac{1}{2w_0b_n}Ai'(f_n)\right], \quad (15)$$

$$M_n = \sqrt{-\frac{\pi}{b_n}}\exp\left(-\frac{c_n^2}{4b_n}+\frac{c_n}{8w_0^3b_n^2}-\frac{1}{96w_0^6b_n^3}\right) \times\left[-\frac{1}{2b_n}Ai(f_n)+\left(\frac{c_n^2}{b_n^2}-\frac{c_n}{w_0^3b_n^3}+\frac{1}{8w_0^6b_n^4}\right)\frac{Ai(f_n)}{4} + \left(-\frac{1}{4w_0^4b_n^3}+\frac{c_n}{w_0b_n^2}\right)\frac{Ai'(f_n)}{2}\right], \quad (16)$$

with

$$b_1 = \frac{i\beta_{2x}}{w_0^2}-\frac{kn_o^2}{2izn_e}, \quad c_1 = \frac{i\beta_{1x}}{w_0}+\frac{kn_o^2x}{izn_e},$$

$$b_2 = \frac{i\beta_{1x}}{w_0^2}-\frac{kn_e}{2iz}, \quad c_2 = \frac{i\beta_{1y}+a}{w_0}+\frac{kn_e y}{iz},$$

$$b_3 = \frac{i\beta_{2y}}{w_0^2}-\frac{kn_o}{2iz}, \quad c_3 = \frac{i\beta_{1y}+a}{w_0}+\frac{kn_o y}{iz},$$

$$b_4 = \frac{i\beta_{2x}}{w_0^2}-\frac{kn_o}{2iz}, \quad c_4 = \frac{i\beta_{1x}+a}{w_0}+\frac{kn_o x}{iz},$$

$$f_1 = \frac{1}{16w_0^4b_1^2}-\frac{c_1}{2w_0b_1}, \quad f_2 = \frac{1}{16w_0^4b_2^2}-\frac{c_2}{2w_0b_2},$$

$$f_3 = \frac{1}{16w_0^4b_3^2}-\frac{c_3}{2w_0b_3}, \quad f_4 = \frac{1}{16w_0^4b_4^2}-\frac{c_4}{2w_0b_4},$$

and $Ai'(\cdots)$ indicates the first-order derivative of the Airy function.

## 3. The numerical calculations and analysis

Based on the analytical expressions for RPCAiBs propagating in uniaxial crystals orthogonal to the optical axis, the propagation properties of RPCAiBs including the influences of the first and the second order chirp factors are further investigated. In the following simulations, the calculation parameters are chosen as $\lambda = 633$ nm, $w_0 = 100$ μm, $a = 0.1$, $n_o = 2.616$, and $Z_r = kw_0^2/2$ is the Rayleigh range.

Comparing the maximum intensity of three components of the beams in Fig. 1, we can find that the intensity of the $z$-component of the beam is much smaller than other components. Therefore, in the following analysis, we ignore the $z$-component and only consider the $x$-component and the $y$-component of the beams. Comparing the maximum intensity of $I_x$ and $I_y$, we can find that before focusing, the minimum value of $I_x$ appears before that of $I_y$, and the minimum value of $I_x$ is larger than that of $I_y$.

To investigate the nonparaxial propagation of the $x$-component of RPCAiBs in uniaxial crystals orthogonal to the optical axis, the intensity evolutions of the beam in different observation planes are depicted in Fig. 2. As shown in Fig. 2,

the propagation trajectory of the beam in the $x$-direction is further than that in the $y$-direction. The maximum intensity of the beam in the $x$-direction is smaller than that in the $y$-direction. Comparing Figs. 2(a1)–2(a4) and Figs. 2(b1)–2(b4), it is obvious that as $\beta_{1x,y}$ increases, the beam is tilted towards the positive $x$-axis and the positive $y$-axis in the $x$-direction and the $y$-direction, respectively, and when $\beta_{1x,y} < 0$, the beam is tilted towards the negative direction. In addition, as $\beta_{1x,y}$ increases, the inclination of the beam in the $x$-direction becomes larger than that in the $y$-direction.

Figure 3 represents the nonparaxial propagation of the $y$-component of RPCAiBs in different observation planes with different first order chirp factors in uniaxial crystal orthogonal to optical axis. It is interesting that the intensity of the beam in the $x$-direction mainly distributes on the main lobe while the intensity of the beam in the $y$-direction mainly distributes on the side lobe. The propagation of the beam in the $x$-direction is much further than that in the $y$-direction. When $\beta_{1x,y}$ increases, the focus position of the beam in the $x$-direction is advanced and the length of the focus of the beam is smaller, as shown in Figs. 3(a1)–3(a4) and Figs. 3(b1)–3(b4). In addition, larger $\beta_{1x,y}$ makes the distribution of the beam more concentrated. Combining Figs. 3(a1)–3(b4) and Figs. 3(a5)–3(b5), it is obvious that the initial slope of the beam in the $x$-direction varies more with $\beta_{1x,y}$ than that in the $y$-direction.

The transverse intensity distributions are plotted to analyze the influence of the first order chirp factor on RPCAiBs. Taking the beams with $\beta_{1x,y} = 5$ as an example, at the start, the intensity mainly distributes on the side lobe as shown in Fig. 4(e1). With the increase of the propagation distance it can be seen that the $x$-component of the beams moves faster than the $y$-component in the $x$-direction, while the $y$-component moves faster than the $x$-component in the $y$-direction in Figs. 4(e2)–4(e4). In addition, a change of $\beta_{1x,y}$ causes the $x$-component of the beams to move more than the $y$-component in the $x$-direction and the $y$-component move more than the $x$-component in the $y$-direction when the propagation distance is equal, as shown in Figs. 4(a2)–4(e4).

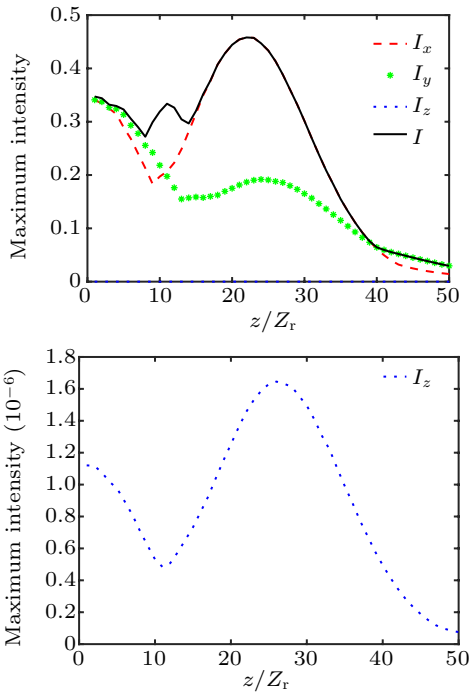



**Fig. 1.** The maximum intensity of radially polarized Airy beams in uniaxial crystals orthogonal to the optical axis with $n_e = 1.5n_o$.

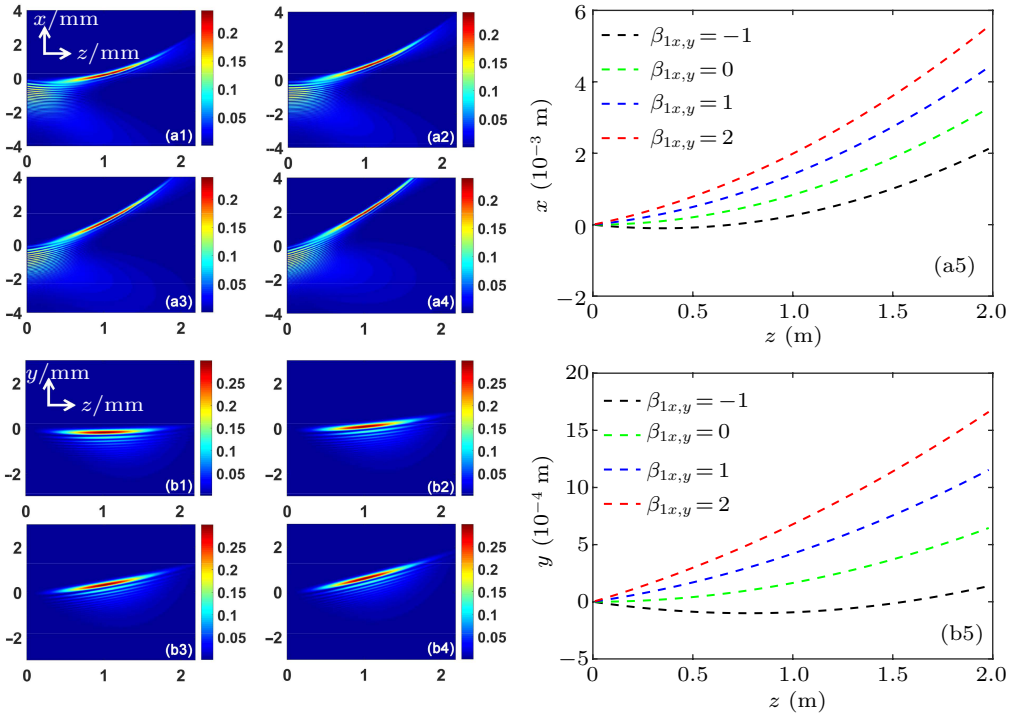



**Fig. 2.** The nonparaxial propagation trajectories and intensity evolutions of the $x$-component of RPCAiBs in different observation planes in uniaxial crystals orthogonal to the optical axis with $n_e = 1.5n_o$ and $\beta_{2x,y} = 0$: (a1) and (b1) $\beta_{1x} = \beta_{1y} = -1$; (a2) and (b2) $\beta_{1x} = \beta_{1y} = 0$; (a3) and (b3) $\beta_{1x} = \beta_{1y} = 1$; (a4) and (b4) $\beta_{1x} = \beta_{1y} = 2$.

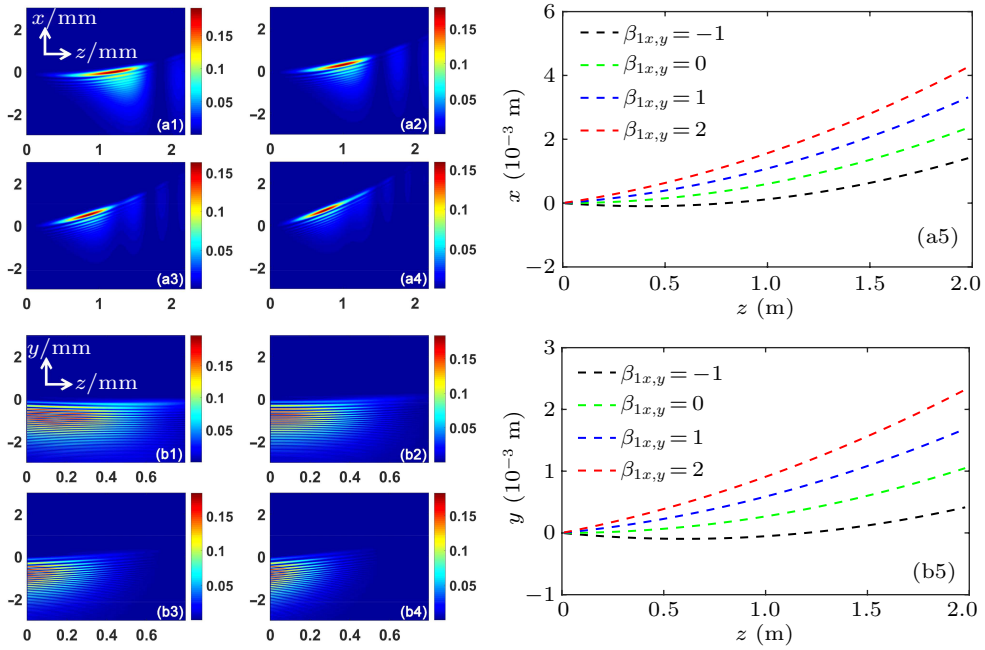



**Fig. 3.** The nonparaxial propagation trajectories and intensity evolutions of the $y$-component of RPCAiBs in different observation planes in uniaxial crystals orthogonal to the optical axis with $n_e = 1.5n_o$ and $\beta_{2x,y} = 0$: (a1) and (b1) $\beta_{1x} = \beta_{1y} = -1$; (a2) and (b2) $\beta_{1x} = \beta_{1y} = 0$; (a3) and (b3) $\beta_{1x} = \beta_{1y} = 1$; (a4) and (b4) $\beta_{1x} = \beta_{1y} = 2$.

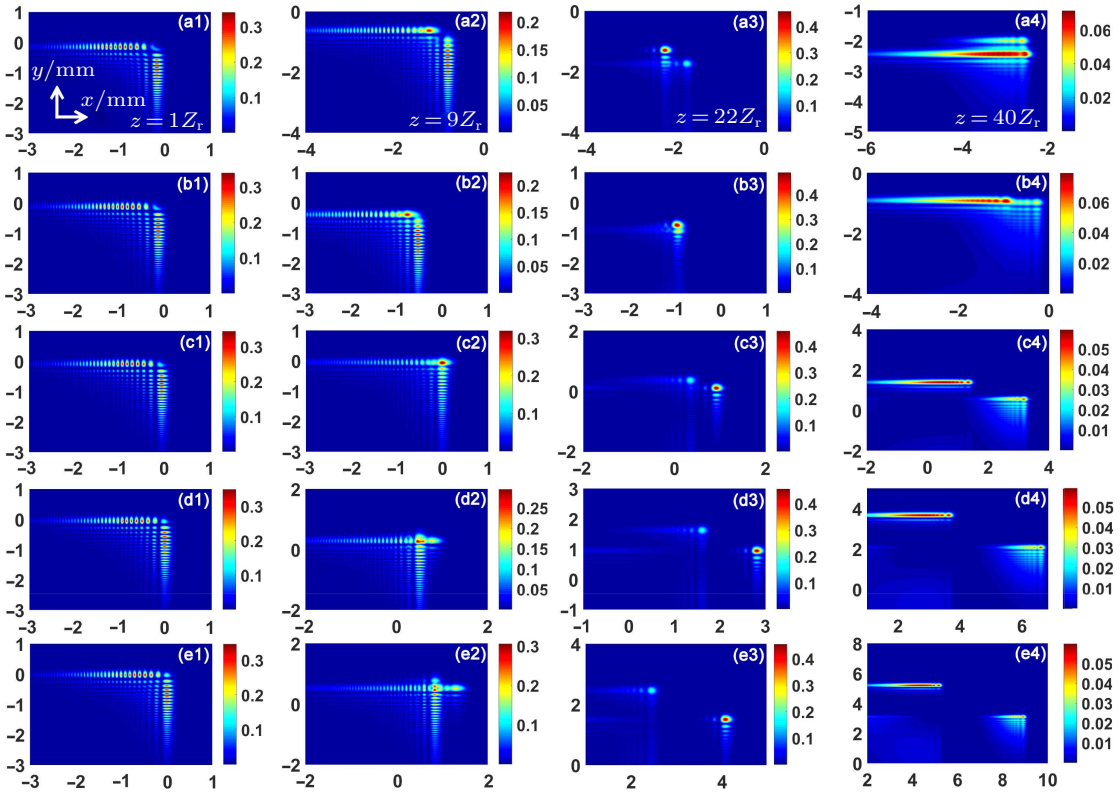



**Fig. 4.** Intensity distributions of RPCAiBs in uniaxial crystals orthogonal to the optical axis with $\beta_{2x,y} = 0$ and $n_e = 1.5n_o$: (a1)–(a4) $\beta_{1x} = \beta_{1y} = -5$; (b1)–(b4) $\beta_{1x} = \beta_{1y} = -3$; (c1)–(c4) $\beta_{1x} = \beta_{1y} = 0$; (d1)–(d4) $\beta_{1x} = \beta_{1y} = 3$; (e1)–(e4) $\beta_{1x} = \beta_{1y} = 5$.

To investigate the nonparaxial propagation of the $x$-component of RPCAiBs in uniaxial crystals orthogonal to the optical axis, the intensity evolutions and the trajectories of the beam in different observation planes are depicted in Fig. 5. Comparing Figs. 5(a2)–5(a4) and Figs. 5(b2)–5(b4), we can find that the maximum intensity of the $x$-component in the $x$-direction varies more with $\beta_{2x,y}$ than that in the $y$-direction. At the same time, with the increase of $\beta_{2x,y}$, the intensity of the side lobe of the beam in the $x$-direction becomes more obvious compared to the main lobe while the intensity of the beam in the $y$-direction has no such phenomenon. Comparing Figs. 5(a5) and 5(b5), one can see that as the $\beta_{2x,y}$ increases, the trajectory of the beam in the $x$-direction changes more than that in the $y$-direction.

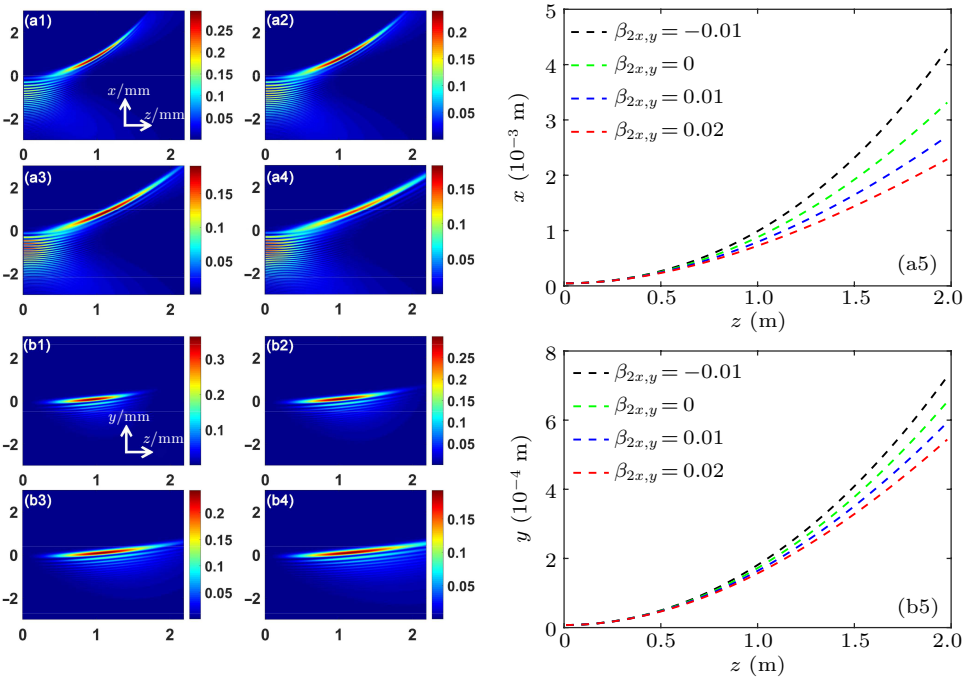



**Fig. 5.** The nonparaxial propagation trajectories and intensity evolutions of the $x$-component of RPCAiBs in different observation planes in uniaxial crystals orthogonal to the optical axis with $n_e = 1.5n_o$ and $\beta_{1x,y} = 0$: (a1) and (b1) $\beta_{2x} = \beta_{2y} = -0.01$; (a2) and (b2) $\beta_{2x} = \beta_{2y} = 0$; (a3) and (b3) $\beta_{2x} = \beta_{2y} = 0.01$; (a4) and (b4) $\beta_{2x} = \beta_{2y} = 0.02$.

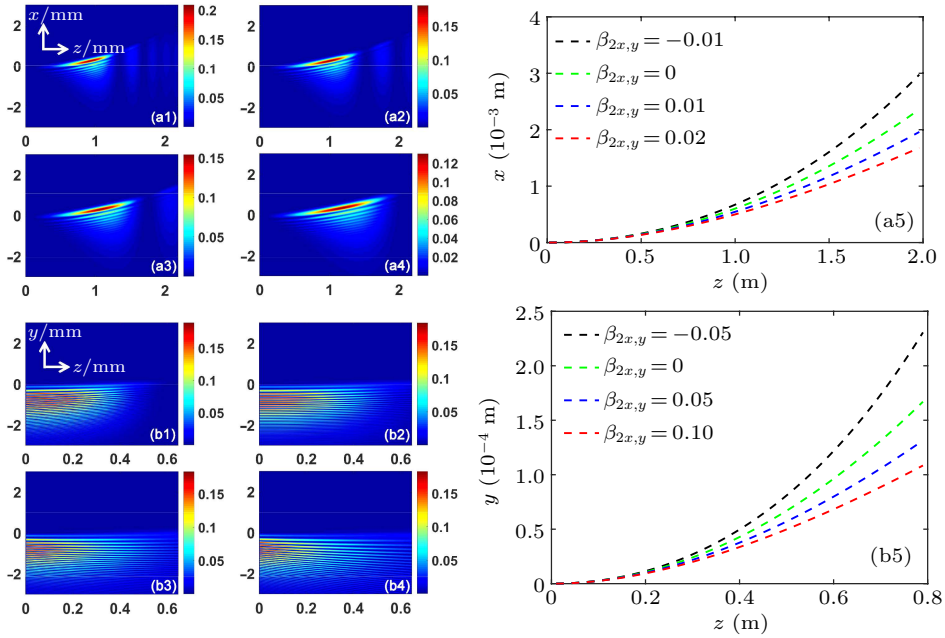



**Fig. 6.** The nonparaxial propagation trajectories and intensity evolutions of the $y$-component of RPCAiBs in different observation planes in uniaxial crystals orthogonal to the optical axis with $n_e = 1.5n_o$ and $\beta_{1x,y} = 0$: (a1) $\beta_{2x} = \beta_{2y} = -0.01$, (b1) $\beta_{2x} = \beta_{2y} = -0.05$; (a2) and (b2) $\beta_{2x} = \beta_{2y} = 0$; (a3) $\beta_{2x} = \beta_{2y} = 0.01$, (b3) $\beta_{2x} = \beta_{2y} = 0.05$; (a4) $\beta_{2x} = \beta_{2y} = 0.02$, (b4) $\beta_{2x} = \beta_{2y} = 0.1$.

To further learn about the variation of the intensity during propagation, the intensity evolutions of the $y$-component of RPCAiBs with different second order chirp factors are depicted. Comparing Figs. 6(a1) and 6(b1), we can derive that the propagation of the beam in the $x$-direction is much further than that in the $y$-direction, and the intensity in the $x$-direction has a focused performance in the main lobe while in the $y$-direction it always distributes on the side lobes. With $\beta_{2x,y}$ becoming larger, the depth of the focus of the beam in the $x$-direction decreases and the length of the focus increases but the maximum intensity of the beam in the $y$-direction is unchanged, as shown in Figs. 6(a1)–6(b4).

In Fig. 7, transverse intensity distributions of RPCAiBs with different second order chirp factors are plotted. Comparing Figs. 7(a2)–7(e2), we can conclude that when $z = 9Zr$, larger $\beta_{2x,y}$ makes the intensity tend to be distributed in the $x$-direction. Moreover, comparing Figs. 7(a2)–7(e4), we can derive that the distance between the $x$- and the $y$-components of RPCAiBs with larger $\beta_{2x,y}$ increases more slowly with the propagation distance increasing.

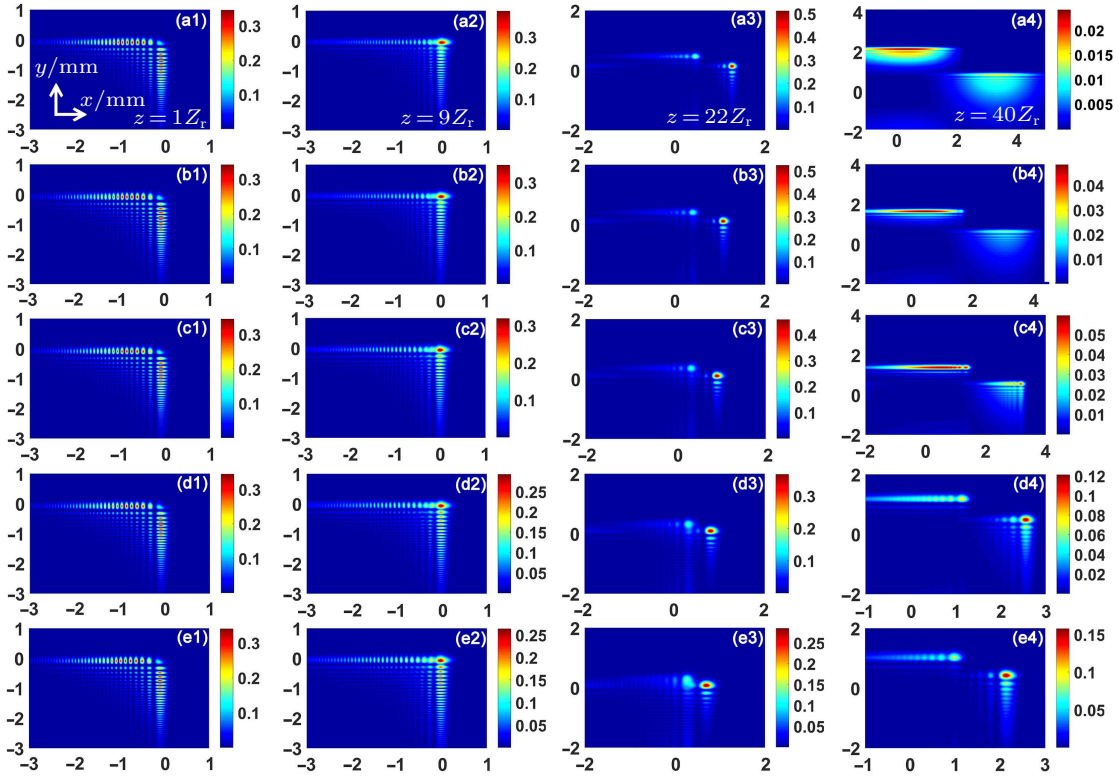



**Fig. 7.** Intensity distributions of RPCAiBs in uniaxial crystals orthogonal to the optical axis with $\beta_{1x,y} = 0$ and $n_e = 1.5n_o$: (a1)–(a4) $\beta_{2x} = \beta_{2y} = -0.02$; (b1)–(b4) $\beta_{2x} = \beta_{2y} = -0.01$; (c1)–(c4) $\beta_{2x} = \beta_{2y} = 0$; (d1)–(d4) $\beta_{2x} = \beta_{2y} = 0.01$; (e1)–(e4) $\beta_{2x} = \beta_{2y} = 0.02$.

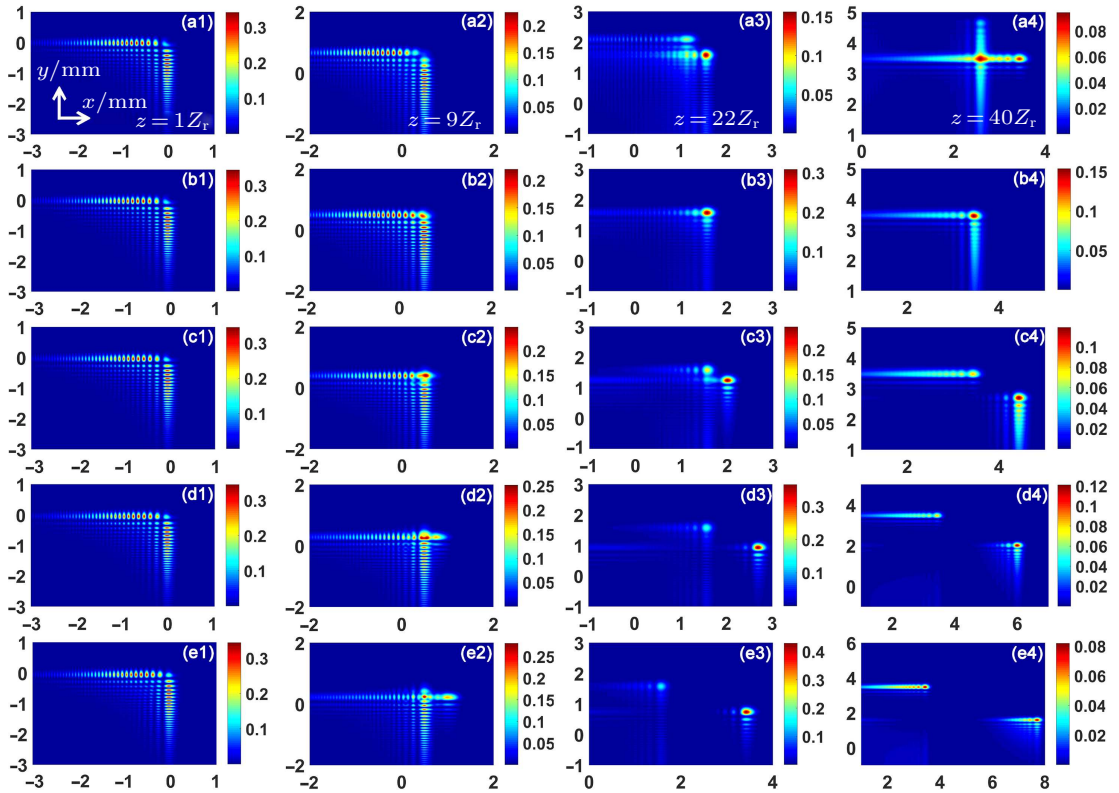



**Fig. 8.** Intensity distributions of RPCAiBs in uniaxial crystals orthogonal to the optical axis with $\beta_{1x,y} = 3$ and $\beta_{2x,y} = 0.01$: (a1)–(a4) $n_e = 0.8n_o$; (b1)–(b4) $n_e = n_o$; (c1)–(c4) $n_e = 1.2n_o$; (d1)–(d4) $n_e = 1.5n_o$; (e1)–(e4) $n_e = 1.8n_o$.

To further learn about the effect of the ratio of $n_e$ to $n_o$ on RPCAiBs, the intensity distributions of the beams are depicted in Fig. 8. Comparing Figs. 8(a1)–8(e4), we can find that the distance between the $x$-component and the $y$-component will increase with the propagation distance increasing when $n_e \neq n_o$. It can be seen in Figs. 8(a1)–8(e2) that only the velocity of the $x$-component in the $x$–$y$ plane is adjusted by the ratio of $n_e$ to $n_o$. In addition, in Figs. 8(a3)–8(e3), when the

ratio of $n_e$ to $n_o$ increases, the intensity of the focus of the $y$-component does not change while that of the $x$-component becomes larger.

## 4. Conclusion

In summary, we have analyzed the propagation evolutions, the trajectories in different observation planes and the transverse intensity of RPCAiBs by deriving analytical expressions of three components of the nonparaxial propagation of RPCAiBs in a uniaxial crystal orthogonal to the optical axis. Although the initial slope of RPCAiBs in both the $x$-direction and the $y$-direction increases as $\beta_{1x}$ and $\beta_{1y}$ become larger, the initial slope of the beams in the $x$-direction increases more. In addition, with $\beta_{1x}$ and $\beta_{1y}$ increasing, the focus position of the $y$-component of RPCAiBs is advanced, the length of the focus becomes smaller and the intensity distribution becomes more concentrated while the $x$-component of RPCAiBs has no difference in these three aspects with larger $\beta_{1x}$ and $\beta_{1y}$. The acceleration of RPCAiBs in both the $x$-direction and the $y$-direction becomes larger with $\beta_{2x}$ and $\beta_{2y}$ increasing, but the acceleration of the beams in the $x$-direction increases more. In addition, the ratio of $n_e$ to $n_o$ can adjust not only the difference of the depth of the focus between the $x$- and the $y$-components but also the difference of the velocity between the $x$- and the $y$-components. We believe this investigation of RPCAiBs will be available for applications of laser processing. It can be expected that the desired shape of the focus and its depth can be achieved by adjusting the first and the second order chirp factors, and the ratio of $n_e$ to $n_o$.

## Acknowledgment

The authors thank Yujun Liu for valuable advice.

## References


[1] Berry M V and Balazs N L 1979 *Am. J. Phys.* **47** 264
[2] Siviloglou G A and Christodoulides D N 2007 *Opt. Lett.* **32** 979
[3] Siviloglou G A, Broky J, Dogariu A and Christodoulides D N 2007 *Phys. Rev. Lett.* **99** 213901
[4] Siviloglou G A, Broky J, Dogariu A and Christodoulides D N 2008 *Opt. Lett.* **33** 207
[5] Broky J, Siviloglou G A, Dogariu A and Christodoulides D N 2008 *Opt. Express* **16** 12880
[6] Efremidis N K, Chen Z G, Segev M and Christodoulides D N 2019 *Optica* **6** 686
[7] Baumgartl J, Mazilu M and Dholakia K 2008 *Nat. Photon.* **2** 675
[8] Vettenburg T, Dalgarno H I, Nylk J, Coll-Lladó C, Ferrier D E, Čižmár T, Gunn-Moore F J and Dholakia K 2014 *Nat. Methods* **11** 541
[9] Abdollahpour D, Suntsov S, Papazoglou D G and Tzortzakis S 2010 *Phys. Rev. Lett.* **105** 253901
[10] Panagiotopoulos P, Papazoglou D G, Couairon A and Tzortzakis S 2013 *Nat. Commun.* **4** 2622
[11] Polynkin P, Kolesik M, Moloney J V, Siviloglou G A and Christodoulides D N 2009 *Science* **324** 229
[12] Polynkin P, Kolesik M and Moloney J 2009 *Phys. Rev. Lett.* **103** 123902
[13] Xu C J, Hu H C, Liu Y J and Deng D M 2020 *Opt. Lett.* **45** 1451
[14] Liu Y J, Xu C J, Lin Z J, Wu Y H, Wu L C and Deng D M 2020 *Opt. Lett.* **45** 2957
[15] Wu Y, Lin Z J, Xu C J, Fu X M, Chen K H, Qiu H X and Deng D M 2020 *Ann. Phys.* **532** 2000188
[16] Xu C J, Wu Y and Deng D M 2020 *Opt. Lett.* **45** 3502
[17] Efremidis N K 2014 *Phys. Rev. A* **89** 023841
[18] Zhang Y Q, Belić M R, Zhang L, Zhong W P, Zhu D Y, Wang R M and Zhang Y P 2015 *Opt. Express* **23** 10467
[19] Zhang Y Q, Liu X, Belić M R, Zhong W P, Wen F and Zhang Y P 2015 *Opt. Lett.* **40** 3786
[20] Li H H, Wang J G, Tang M M, Cao J X and Li X Z 2018 *Opt. Commun.* **427** 147
[21] Li H H, Tang M M, Wang J G, Cao J X and Li X Z 2019 *Appl. Phys. B* **125** 51
[22] Li H H, Wang J G, Tang M M and Li X Z 2018 *J. Mod. Opt.* **65** 314
[23] Li H H, Wang J G, Tang M M and Li X Z 2017 *J. Opt. Soc. Am. A* **34** 1114
[24] Li H H, Wang J G, Tang M M and Li X Z 2017 *J. Mod. Opt.* **64** 2363
[25] Zhang L F, Liu K, Zhong H Z, Zhang J G, Li Y and Fan D Y 2015 *Opt. Express* **23** 2566
[26] Driben R, Konotop V V and Meier, T 2014 *Opt. Lett.* **39** 5523
[27] Liu Y J, Xu C J, Wu L C and Deng D M 2020 *Opt. Commun.* **454** 124494
[28] Ciattoni A, Crosignani B and Porto P D 2001 *J. Opt. Soc. Am. A* **18** 1656
[29] Ciattoni A, Cincotti G and Palma C 2002 *J. Opt. Soc. Am. A* **19** 1422
[30] Ciattoni A and Palma C 2003 *J. Opt. Soc. Am. A* **20** 2163
[31] Laabs H 1998 *Opt. Commun.* **147** 1
[32] Agrawal G P and Pattanayak D N 1979 *J. Opt. Soc. Am.* **69** 575
[33] Duan K L and Lü B D 2003 *Opt. Express* **11** 1474
[34] Deng D M and Guo Q 2009 *J. Opt. Soc. Am. B* **26** 2044
[35] Born M and Wolf E 2013 *Principles of optics: electromagnetic theory of propagation, interference and diffraction of light* (Amerstam: Elsevier)
[36] Li D D, Peng X, Peng Y L, Zhang L P and Deng D M 2017 *J. Opt. Soc. Am. B* **34** 891
[37] Deng D M and Guo Q 2007 *Opt. Lett.* **32** 2711
[38] Zhan Q 2009 *Adv. Opt. Photon.* **1** 1
[39] Hnatovsky C, Shvedov V, Krolikowski W and Rode A 2011 *Phys. Rev. Lett.* **106** 123901
[40] Novotny L, Beversluis M R, Youngworth K S and Brown T G 2001 *Phys. Rev. Lett.* **86** 5251
[41] Varin C and Piché M 2002 *Appl. Phys. B* **74** s83
[42] Salamin Y I 2007 *Opt. Lett.* **32** 90
[43] Nesterov A V and Niziev V G 2000 *J. Phys. D* **33** 1817
[44] Niziev V G and Nesterov A V 1999 *J. Phys. D* **32** 1455
[45] Kuga T, Torii Y, Shiokawa N, Hirano T, Shimizu Y and Sasada H 1997 *Phys. Rev. Lett.* **78** 4713
[46] Gahagan K T and Swartzlander G A 1999 *J. Opt. Soc. Am. B* **16** 533
[47] Min C J, Shen Z, Shen J F, Zhang Y Q, Fang H, Yuan G H, Du L P, Zhu S W, Lei T and Yuan X C 2013 *Nat. Commun.* **4** 2891
[48] Zhong T F, Zhang J B, Feng L Y, Pang Z H, Wang L Y and Deng D M 2018 *J. Opt. Soc. Am. B* **35** 1354
[49] Yang Q, Zhu W Z, Xu C J, Lu M Y, Chen X P, Deng D M and Huang L Q 2019 *J. Opt. Soc. Am. A* **36** 994
[50] Wu X L, Xie J T and Deng D M 2019 *Appl. Phys. B* **125** 87
[51] Xie J T, Zhang J B, Zheng X T, Ye J R and Deng D M 2018 *Opt. Express* **26** 11309
[52] Khonina S N, Alferov S V and Karpeev S V 2013 *Opt. Lett.* **38** 3223
[53] Khonina S N and Kharitonov S I 2015 *J. Mod. Opt.* **62** 125
[54] Wang H F, Shi L P, Lukyanchuk B S, Sheppard C J R and Chong C T 2008 *Nat. Photon.* **2** 501
[55] Fadeyeva T A, Shvedov V G, Izdebskaya Y V, Volyar A V, Brasselet E, Neshev D N, Desyatnikov A S, Krolikowski W and Kivshar Y S 2010 *Opt. Express* **18** 10848
[56] Khonina S N, Porfirev A P and Kazanskiy N L 2020 *Sci. Rep.* **10** 5590
[57] Chremmos I, Efremidis N K and Christodoulides D N 2011 *Opt. Lett.* **36** 1890
[58] Khonina S N, Porfirev A P and Ustinov A V 2018 *J. Opt.* **20** 025605
[59] Li J S, Gao X M, Zhuang S L and Huang C Q 2010 *Optik* **121** 821
[60] Khonina S N, Ustinov A V and Porfirev A P 2019 *J. Opt. Soc. Am. A* **36** 1039
[61] Gradshteyn I S and Ryzhik I M 2014 *Table of integrals, series, and products* (New York: Academic)